

## High-Field Magnetization Study of $R_2\text{Fe}_{17}\text{N}_2$ ( $R = \text{Ho}$ and Er) Nitrides

I. S. Tereshina<sup>1</sup> · E. A. Tereshina-Chitrova<sup>2</sup> ·  
I. A. Pelevin<sup>3</sup> · M. Doerr<sup>4</sup> · J. M. Law<sup>5</sup> ·  
V. N. Verbetski<sup>6</sup> · A. A. Salamova<sup>6</sup>

Received: 21 September 2017 / Accepted: 27 November 2017 / Published online: 1 December 2017  
© Springer Science+Business Media, LLC, part of Springer Nature 2017

**Abstract** The structure and magnetic properties of the nitrated compounds  $R_2\text{Fe}_{17}\text{N}_2$  ( $R = \text{Ho}$  and Er) are studied. The type of crystal structure  $\text{Th}_2\text{Ni}_{17}$  is preserved upon nitrogenation, and the relative unit cell volume  $\Delta V/V$  increase exceeds 6%. Magnetic studies are performed in fields up to 60 T at 4.2 K on aligned powder samples. Field-induced spin-reorientation (SR) transitions are observed in the  $M(H)$  curves of  $R_2\text{Fe}_{17}\text{N}_2$ . Unlike the parent  $R_2\text{Fe}_{17}$  compounds, where the magnetization increases in steps as the field grows stronger,  $R_2\text{Fe}_{17}\text{N}_2$  demonstrate a gradual increase in magnetization. It is indicative of the change of the SR transition from first to the second type. Extrapolation of magnetization curves to the theoretical value of magnetization in the forced ferromagnetic state yields the coefficient of the inter-sublattice R–Fe exchange interaction. The inter-sublattice exchange is found to decrease upon nitrogenation.

**Keywords** Rare earth intermetallics · High magnetic fields · Permanent magnet materials · Nitrides · Low temperatures

---

✉ I. S. Tereshina  
tereshina@physics.msu.ru

<sup>1</sup> Department of Physics, Lomonosov Moscow State University, Moscow, Russia

<sup>2</sup> Institute of Physics CAS, Prague, Czech Republic

<sup>3</sup> Baikov Institute of Metallurgy and Materials Science RAS, Moscow, Russia

<sup>4</sup> Technische Universität Dresden, Dresden, Germany

<sup>5</sup> Dresden High Magnetic Field Laboratory (HLD-EMFL), Helmholtz-Zentrum Dresden-Rossendorf, Dresden, Germany

<sup>6</sup> Department of Chemistry, Lomonosov Moscow State University, Moscow, Russia

## 1 Introduction

The rare earth (*R*) intermetallics with a high Fe content are the keystone of hard magnetic materials. They possess the magnetic properties necessary for the wide spectrum of industrial applications [1, 2]. In the past years, the worldwide scientific community strived for finding the alternative for the *R*-containing alloys and/or to decrease the amount of *R* metals in existing alloys with the aim of decreasing cost of final materials. No significant advance in this field has been reached so far. Therefore, tuning of the composition by using various doping elements as well as deeper studies of the fundamental and functional properties of materials still remain topical subjects. Favorable results are also facilitated by improved experimental methods, which allow us to obtain new, thorough experimental data. Attainment of desired magnetic characteristics is possible only in the case of materials with the easy-axis type of magnetic anisotropy (MA).

Iron-rich  $R_2Fe_{17}$  intermetallics and their nitrides (as well as hydrides and carbides) with light rare earths crystallize in the rhombohedral  $Th_2Zn_{17}$  crystal structure, while those with heavy *R*s have a hexagonal  $Th_2Ni_{17}$  crystal structure (Fig. 1). The magnetic anisotropy of  $R_2Fe_{17}$  is of the easy-plane type in the whole range of magnetic ordering in all of the compounds but  $Tm_2Fe_{17}$  (in the latter case, the easy axis is due to the prevailing uniaxial *Tm* MA at low temperatures). The required easy axis MA can be obtained by interstitial doping of  $R_2Fe_{17}$  [3, 4]. Although the uniaxial MA was usually observed at low temperatures and only for some of the doped compounds, strong room temperature easy axis magnetic anisotropy was successfully stabilized in  $Sm_2Fe_{17}N_{3-x}$  and  $Sm_2Fe_{17}C_{3-x}$  [2, 5, 6]. Interestingly enough, a trihydride  $Tb_2Fe_{17}H_3$  also showed a room temperature uniaxial MA [7, 8].

As a rule, impurity atoms of nitrogen, hydrogen or carbon locate interstitially and do not change the crystal structure type while increasing the unit cell volume [9–12]. According to the literature [10, 11], compounds  $R_2Fe_{17}$  can absorb up to 5 atoms of hydrogen and 3 atoms of nitrogen or carbon per formula unit (f.u.). Magnetic structures of  $R_2Fe_{17}(N, C, H)_x$  can be described by non-rigidly coupled rare earth and 3d magnetic sublattices, which order either parallel or antiparallel to each other in the case of light and heavy rare earths, respectively [13]. The magnetism of the 3d sublattice is

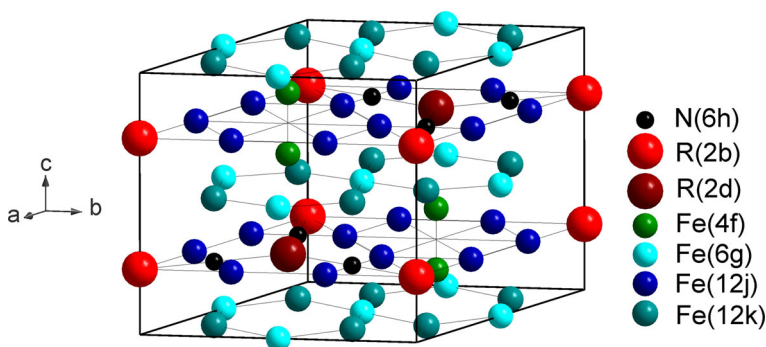


**Fig. 1** Hexagonal crystal structure of the  $Th_2Ni_{17}$  type for nitrogenated  $R_2Fe_{17}$  (Color figure online)

usually studied using compounds with non-magnetic rare earths such as Y or Lu [2, 14–20]. The use of high magnetic fields allows us to estimate the magnetic anisotropy field [21–23] in highly anisotropic compounds and more importantly, to observe the change of magnetic structures of ferrimagnetically ordered  $R_2\text{Fe}_{17}(\text{N}, \text{C}, \text{H})_x$  triggered by an applied magnetic field. Observations of various field-induced spin-reorientation transitions [24–26], or transitions from ferri- to the ferromagnetic state [27] and determination of the inter-sublattice exchange [28–33] are the advantages of the high-field experiments. The goal of the present work is to study the influence of nitrogen absorption on structural and magnetic properties of  $R_2\text{Fe}_{17}\text{N}_2$  with Ho and Er. These rare earths were chosen due to the different signs of the Stevens'  $\alpha_J$  factor ( $\alpha_J > 0$  for  $\text{Er}^{3+}$  and  $\alpha_J < 0$  for  $\text{Ho}^{3+}$ ) [34]. For this reason, we expect to observe results directly related to the specific features of the 4f ions.

## 2 Experimental Details

The parent samples of  $\text{Ho}_2\text{Fe}_{17}$  and  $\text{Er}_2\text{Fe}_{17}$  were obtained as described in Ref. [16]. Nitrides were produced at 450 °C in a molecular  $\text{N}_2$  atmosphere under the pressure of 10 bar. Prior to the nitrogenation procedure, the samples were crushed into powder having particles size not exceeding 5  $\mu\text{m}$ . It allowed us to obtain samples homogenous in nitrogen content. The amount of absorbed nitrogen was calculated using a Van der Waals equation  $p(V - nb) = nRT$ , where  $b$  is a Van der Waals' coefficient equal to 38.6  $\text{cm}^3/\text{mole}$ ;  $p$  is a nitrogen pressure in the system, in atm.;  $R$  is the universal gas constant  $82 \times 10^6 \text{ cm}^3 \text{ atm}/(\text{mole K})$ ;  $V$  is a volume of nitrogen, in  $\text{cm}^3$ ;  $T$  is temperature, in K;  $n$  is the amount of nitrogen, in mole. Nitrided compounds with 2 nitrogen atoms per formula unit (f.u.) were obtained in this work. Precision in the nitrogen content determination was 0.1 at.N/f.u.

The structural studies were carried out using powder X-ray diffraction (XRD) on a DRON-3M diffractometer in a Cu radiation. The magnetic study was performed on powder samples. Samples were oriented at room temperature in a rotating magnetic field since their magnetic anisotropy is planar. Powder samples were fixed using a non-magnetic epoxy resin (similar approach was used for the 2–17 samples in Ref. [14]). The Curie temperatures and spin-reorientation transition temperatures were determined using a thermomagnetic analysis.

The samples were measured in steady and pulsed magnetic fields. First, the magnetization curves for all of  $R_2\text{Fe}_{17}\text{N}_2$  were measured at 4.2 K in fields up to 14 T applied along the  $c$  axis and in the basal plane (perpendicularly to the  $c$  axis) using a PPMS-14 magnetometer (Quantum Design, USA). After that, a high-field magnetization study in magnetic fields up to 60 T at 4.2 K was performed using a pulsed field magnet (20-ms pulse duration) at the High-Field Laboratory of Dresden [35]. All pulsed field data were calibrated against the magnetization measured in steady fields. All magnetization data presented below were corrected for demagnetization.

**Table 1** Structural and magnetic parameters of the parent and nitrogenated compounds  $R_2\text{Fe}_{17}\text{N}_x$  ( $R = \text{Ho}$  and  $\text{Er}$ ,  $x = 0$  and  $2$ )

| Compound                              | $a$ (Å) | $c$ (Å) | $V$ (Å <sup>3</sup> ) | $\Delta V/V$ (%) | $c/a$ | $T_C$ (K) | $T_{SR}$ (K) |
|---------------------------------------|---------|---------|-----------------------|------------------|-------|-----------|--------------|
| $\text{Ho}_2\text{Fe}_{17}$           | 8.442   | 8.311   | 512.3                 | –                | 0.984 | 327       | –            |
| $\text{Ho}_2\text{Fe}_{17}\text{N}_2$ | 8.608   | 8.480   | 543.5                 | 6.1              | 0.985 | 695       | –            |
| $\text{Er}_2\text{Fe}_{17}$           | 8.441   | 8.251   | 508.5                 | –                | 0.977 | 296       | –            |
| $\text{Er}_2\text{Fe}_{17}\text{N}_2$ | 8.610   | 8.428   | 540.4                 | 6.4              | 0.978 | 665       | 120          |

### 3 Results and Discussion

The X-ray powder diffraction analysis confirmed the hexagonal crystal structure of  $\text{Th}_2\text{Ni}_{17}$  type for both parent  $\text{Ho}_2\text{Fe}_{17}$  and  $\text{Er}_2\text{Fe}_{17}$  compounds as well as for their nitrides  $\text{Ho}_2\text{Fe}_{17}\text{N}_2$  and  $\text{Er}_2\text{Fe}_{17}\text{N}_2$ . The materials were identified as single phase (the amount of  $\alpha$ -Fe is less than 3 at%). Crystallographic data for the alloys are presented in Table 1. The unit cell volume was found to expand by more than 6% upon nitrogenation. Table 1 also shows the Curie temperatures and spin-reorientation transition temperatures for the samples. All structural and magnetic parameters agree well with the available literature data [2].

Figures 2 and 3 demonstrate the magnetization curves measured in pulsed magnetic fields up to 60 T and in steady magnetic fields up to 14 T for  $\text{Ho}_2\text{Fe}_{17}\text{N}_2$  and  $\text{Er}_2\text{Fe}_{17}\text{N}_2$ . For comparison, insets in Figs. 2 and 3 show data adopted from Refs. [24, 26] for the parent single-crystalline samples  $\text{Ho}_2\text{Fe}_{17}$  and  $\text{Er}_2\text{Fe}_{17}$ , respectively. It is worth noting that all magnetization measurements were conducted upon increasing and decreasing field (we do not show the latter in order to keep the figures clear). It is seen that both parent materials possess the anisotropy of the easy-plane type at 4.2 K with the  $c$  axis (crystallographic direction [001]) being the hard magnetization direction (HMD). It is known that Er magnetic moments lie along the  $c$  axis in  $\text{Er}_2\text{Fe}_{17}$ , while the Fe sublattice' magnetic moments have preference for the basal plane [14]. The easy-plane Fe anisotropy dominates in the whole range of magnetic ordering, hence the observed easy-plane type of magnetic anisotropy in the  $\text{Er}_2\text{Fe}_{17}$  compound. Negative Stevens'  $\alpha_J$  factor in  $\text{Ho}^{3+}$  is the reason for the same sign of anisotropies of the rare earth and Fe sublattices resulting in the magnetic anisotropy of the easy-plane type in  $\text{Ho}_2\text{Fe}_{17}$ .

As seen from the inset in Fig. 2, magnetization curves of a  $\text{Ho}_2\text{Fe}_{17}$  single crystal measured in the basal plane along the [100] and [120] directions feature sharp field-induced spin-reorientation transitions. Here, we only show the  $M(H)$  curves measured in the increasing magnetic field; however, a small hysteresis was observed upon the decreasing field in Ref. [24]. Since the sublattices' magnetization vectors rotation occurs as the magnetization jumps with a field hysteresis, the transitions are of the first order. Nitrogenation does not influence the type of magnetic anisotropy, which remains of the easy-plane type (Fig. 2). High-field magnetization jumps present in the  $M(H)$  curves of the parent compound are no longer seen for the nitrided  $\text{Ho}_2\text{Fe}_{17}\text{N}_2$  material. We only observe a gradual increase in magnetization both along the [001]

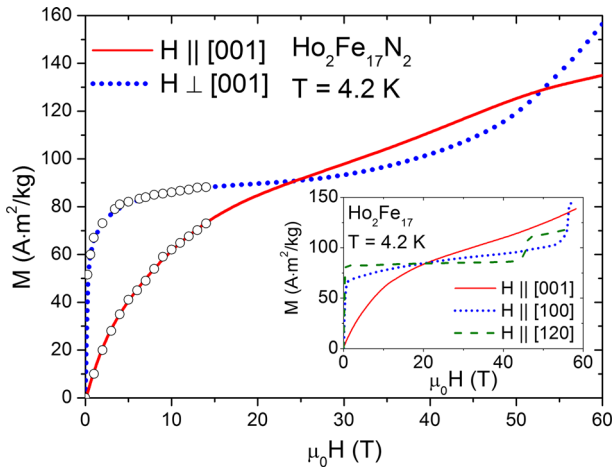


**Fig. 2** Magnetization curves for  $\text{Ho}_2\text{Fe}_{17}\text{N}_2$  aligned powders measured in pulsed magnetic fields at 4.2 K (circles show the steady field data). The inset: the same for the single-crystalline  $\text{Ho}_2\text{Fe}_{17}$  adopted from Ref. [24] (Color figure online)

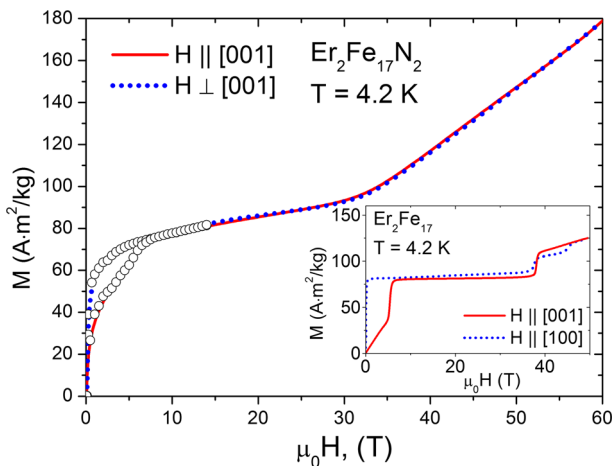


**Fig. 3** Magnetization curves for  $\text{Er}_2\text{Fe}_{17}\text{N}_2$  aligned powders measured in pulsed magnetic fields at 4.2 K (circles show the steady field data). The inset: the same for the single-crystalline  $\text{Er}_2\text{Fe}_{17}$  adopted from Ref. [26] (Color figure online)

direction and perpendicular to it. The magnetic anisotropy field increases from 20 to 25 T.

$\text{Er}_2\text{Fe}_{17}$  displays first-order magnetization transitions both along the easy magnetization direction (EMD) [100] and along the HMD [001] (see inset in Fig. 3) [26]. In the nitrated  $\text{Er}_2\text{Fe}_{17}\text{N}_2$ , the high-field transitions become smooth and non-hysteretic. Here, we observe the change of the order of transition from first to the second order (Fig. 3). Note that the magnetization curves of the nitrated sample at the increasing and decreasing field coincide with each other.

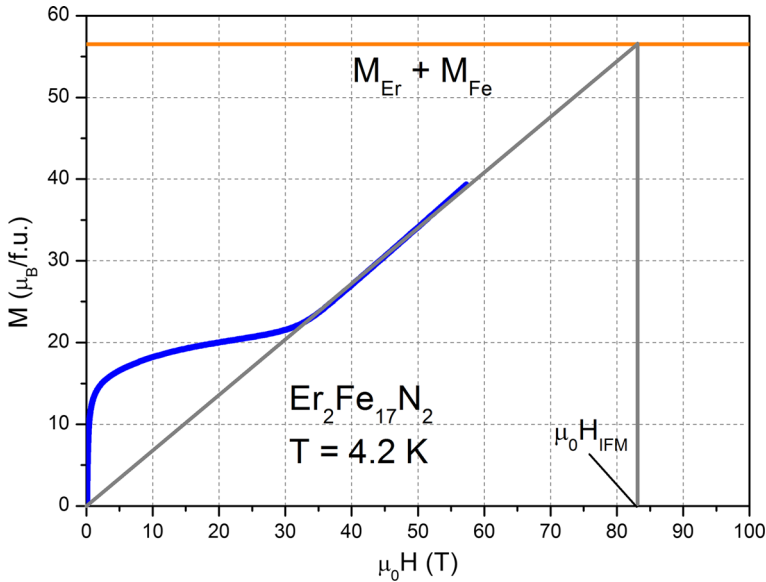


**Fig. 4** Magnetization curve for  $\text{Er}_2\text{Fe}_{17}\text{N}_2$  measured along the easy magnetization direction in pulsed magnetic field up to 60 T at 4.2 K and extrapolation of the curve to the magnetization of the forced ferromagnetic state ( $M_{\text{Er}} + M_{\text{Fe}}$ ) (Color figure online)

The magnetic anisotropy in  $\text{Er}_2\text{Fe}_{17}\text{N}_2$  changes from planar to the cone-of-easy-axes type. Nitrogen atoms occupy interstitial positions 6h (Fig. 1) in the basal plane of the  $\text{Th}_2\text{Ni}_{17}$  type of crystal structure and change gradient of electric field in the vicinity of the  $\text{Er}^{3+}$  ion ( $\alpha_J > 0$  Stevens’ factor). They reorient a quadrupole moment (and the co-aligned magnetic moment) of the rare earth ion toward the  $c$  axis. The influence of nitrogeneration (as well as hydrogenation) on the magnetocrystalline anisotropy of  $R_2\text{Fe}_{17}$  compounds was studied in detail in Refs. [3,22].

In order to obtain information on the inter-sublattice interactions, we first made an estimation of the value of magnetization of all studied compounds based on the two-sublattice model in the field-induced ferromagnetic state (IFM). The latter means that the R and Fe moments are co-directed and can be summed up to the total magnetization. The magnetization of the Fe sublattice was taken equal to  $38.5 \mu_B/\text{f.u.}$ , i.e., the same as in the  $\text{Y}_2\text{Fe}_{17}\text{N}_2$  compound (Lu-containing analogous compound would provide the same value of the Fe magnetization [2]). We assume that the Ho and Er magnetic moments in the ground state of  $R_2\text{Fe}_{17}\text{N}_2$  are equal to their free-ion  $\text{Ho}^{3+}$  and  $\text{Er}^{3+}$  values  $10 \mu_B$  and  $9 \mu_B$ , respectively. Since the magnetization in the ferrimagnetic  $\text{Ho}_2\text{Fe}_{17}\text{N}_2$  is  $18.5 \mu_B/\text{f.u.}$ , then the ferromagnetic  $\text{Ho}_2\text{Fe}_{17}\text{N}_2$  will have  $58.5 \mu_B/\text{f.u.}$  Similarly, we obtain the magnetization of the ferromagnetic  $\text{Er}_2\text{Fe}_{17}\text{N}_2$  as  $56.5 \mu_B/\text{f.u.}$  since in the ferrimagnetic state  $\text{Er}_2\text{Fe}_{17}\text{N}_2$  has  $20.5 \mu_B/\text{f.u.}$

Considering mutual resemblance of the high-field behavior of the  $M(H)$  curves measured in the crystallographic directions perpendicular to each other in  $\text{Er}_2\text{Fe}_{17}\text{N}_2$  (Fig. 4), we assumed that the compound is isotropic at these fields. Moreover, the high-field region of  $M(H)$  curve extrapolates linearly to zero field. Therefore, the

magnetization curve can be analyzed using the method described in detail in Ref. [31]. To determine the value of  $\mu_0 H_{\text{IFM}}$ , we also extrapolated the experimental curve to the magnetization of  $\text{Er}_2\text{Fe}_{17}\text{N}_2$  in the ferromagnetic state (Fig. 4). The extrapolation showed that in order to induce the ferromagnetic state,  $\text{Er}_2\text{Fe}_{17}\text{N}_2$  should be placed into the field of  $\mu_0 H_{\text{IFM}} = 83 \text{ T}$ . The parameter of the inter-sublattice exchange interaction was calculated using the following expression

$$n_{\text{RFe}} = (\mu_0 H_{\text{IFM}} - \mu_0 H_0) / \{(M_{\text{Er}} + M_{\text{Fe}}) - |M_{\text{Er}} - M_{\text{Fe}}|\},$$

where  $\mu_0 H_0$  is a saturation field for the ferrimagnetic sample. Earlier, in Ref. [31] the coupling constant— $J_{\text{ErFe}}/k_{\text{B}}$  (in K)—estimated for the single crystal  $\text{Er}_2\text{Fe}_{17}$  was found to have a value 6.4 K (magnetization of the Fe sublattice,  $M_{\text{Fe}} = 35.5 \mu_{\text{B}}/\text{f.u.}$  [36,37]). Our estimate of the coupling constant of  $\text{Er}_2\text{Fe}_{17}\text{N}_2$ , 6.0 K, means that the inter-sublattice exchange has weakened for more than 6% when the two atoms of nitrogen were inserted into the crystal lattice of  $\text{Er}_2\text{Fe}_{17}$ . In Ref. [31], they also provide the value of  $J_{\text{ErFe}}/k_{\text{B}} = 6.8 \text{ K}$  for  $\text{Ho}_2\text{Fe}_{17}$ . Our estimation for  $\text{Ho}_2\text{Fe}_{17}\text{N}_2$  provides a somewhat lower value. We therefore plan to perform additional measurements including those on free powders.

## 4 Conclusion

In this work, the structure and magnetic properties of nitrides with a high content of Fe  $R_2\text{Fe}_{17}\text{N}_2$  with  $R = \text{Ho}$  and  $\text{Er}$  were investigated. The XRD study on  $R_2\text{Fe}_{17}\text{N}_2$  conducted at room temperature showed the increase in the unit cell volume for more than 6% upon nitrogenation. The magnetic properties were studied with the use of high magnetic fields up to 60 T. We show that the type of magnetocrystalline anisotropy in the  $R_2\text{Fe}_{17}$  compounds can be preserved ( $\text{Ho}_2\text{Fe}_{17}\text{N}_2$ ) or changed ( $\text{Er}_2\text{Fe}_{17}\text{N}_2$ ) upon nitrogenation. While  $\text{Er}_2\text{Fe}_{17}$  has the anisotropy of the easy-plane type,  $\text{Er}_2\text{Fe}_{17}\text{N}_2$  demonstrates a cone of easy axes at  $T = 4.2 \text{ K}$ . Strong influence of nitrogenation on the high-field spin-reorientation transitions is revealed in the course of high-field magnetic experiments. Nitrogen-doped  $\text{Ho}_2\text{Fe}_{17}$  and  $\text{Er}_2\text{Fe}_{17}$  do not demonstrate magnetization jumps as compared to the parent materials and only show a smooth growth of magnetization with the increasing field. For both nitrogen-doped compounds, R–Fe exchange interaction becomes weaker. It was shown that the nitrated  $\text{Er}_2\text{Fe}_{17}$  is isotropic at high fields. We estimate the inter-sublattice coupling constant in  $\text{Er}_2\text{Fe}_{17}\text{N}_2$  as 6.0 K (cf. 6.4 K for  $\text{Er}_2\text{Fe}_{17}$ ).

**Acknowledgements** The work is supported by the Russian Foundation for Basic Research (RFBR) Grant No. 16-03-00612.

## References

1. K.H.J. Buschow, in *Handbook of Magnetic Materials*, vol. 10, ed. by K.H.J. Buschow (North-Holland, Amsterdam, 1997), p. 463
2. H. Fujii, H. Sun, in *Handbook of Magnetic Materials*, vol. 9, ed. by K.H.J. Buschow (North-Holland, Amsterdam, 1995), p. 304

3. I.S. Tereshina, S.A. Nikitin, V.N. Verbetsky, A.A. Salamova, J. Alloys Compd. **336**, 36 (2002)
4. S. Nikitin, I. Tereshina, E. Tereshina, W. Suski, H. Drulis, J. Alloys Compd. **451**, 477 (2008)
5. J.M.D. Coey, H. Sun, J. Magn. Magn. Mater. **87**, L251 (1990)
6. H. Nakayama, K. Takagi, K. Ozaki, K. Kobayashi, Mater. Trans. **53**(11), 1962 (2012)
7. E.A. Tereshina, H. Drulis, Y. Skourski, I.S. Tereshina, Phys. Rev. B. **87**, 214425(5) (2013)
8. G.S. Burkhanov, I.S. Tereshina, I.A. Pelevin, E.A. Tereshina, Dokl. Phys. **58**(12), 528 (2013)
9. V.I. Voronin, A.V. Zinin, N.V. Kudrevatykh, A.N. Pirogov, J. Alloys Compd. **266**, 39 (1998)
10. O. Isnard, S. Miraglia, J.L. Soubeyroux, D. Fruchart, P. l'Héritier, J. Magn. Magn. Mater. **137**, 151 (1994)
11. O. Isnard, S. Miraglia, C. Kolbeck, E. Tomey, J.L. Soubeyroux, D. Fruchart, M. Guillot, C. Rillo, J. Alloys Compd. **178**, 15 (1992)
12. N.M. Hong, Phys. B **226**, 391 (1996)
13. S.S. Jaswal, W.E. Yelon, G.C. Hadjipanayis, Y.Z. Wang, D.J. Sellmyer, Phys. Rev. Lett. **67**(5), 644 (1991)
14. S. Brennan, R. Skomski, O. Cugat, J.M.D. Coey, J. Magn. Magn. Mater. **140–144**, 971 (1995)
15. T. Beuerle, M. Fähnle, Phys. Stat. Sol. (B) **174**, 257 (1992)
16. S.A. Nikitin, E.A. Ovtchenkov, I.S. Tereshina, V.N. Verbetsky, A.A. Salamova, J. Magn. Magn. Mater. **195**, 464 (1999)
17. S.A. Nikitin, I.S. Tereshina, N.Y. Pankratov, E.A. Tereshina, Y.V. Skourski, K.P. Skokov, Y.G. Pastushenkov, Phys. Solid State **43**(9), 1720 (2001)
18. A.G. Kuchin, W. Iwasieczko, H. Drulis, J. Alloys Compd. **480**, 23 (2009)
19. W. Iwasieczko, N.Yu. Pankratov, E.A. Tereshina, S.A. Nikitin, I.S. Tereshina, K.P. Skokov, A.Yu. Karpenkov, R.M. Grechishkin, H. Drulis, J. Alloys Compd. **587**, 739 (2014)
20. E.A. Tereshina, H. Yoshida, A.V. Andreev, I.S. Tereshina, K. Koyama, J. Phys. Soc. Jpn. **76 A**, 82 (2007)
21. O. Isnard, S. Miraglia, M. Guillot, D. Fruchart, J. Appl. Phys. **75**(10), 5988 (1994)
22. I.S. Tereshina, S.A. Nikitin, K.P. Skokov, T. Palewski, V.V. Zubenko, I.V. Telegina, V.N. Verbetsky, A.A. Salamova, J. Alloys Compd. **350**, 264 (2003)
23. G.S. Burkhanov, I.S. Tereshina, M.A. Paukov, I.A. Pelevin, S.A. Nikitin, R. Bezdushnyi, R. Damianova, E.A. Tereshina, H. Drulis, Dokl. Phys. Chem. **469**(1), 102 (2016)
24. Y. Skourski, M.D. Kuz'min, K.P. Skokov, A.V. Andreev, J. Wosnitza, Phys. Rev. B **83**, 214420 (2011)
25. I.S. Tereshina, M. Doerr, Y. Skourski, E.A. Tereshina, K. Watanabe, I.V. Telegina, H. Drulis, IEEE Trans. Magn. **47**(10), 3617 (2011)
26. R. Verhoef, F.R. de Boer, S. Sinnema, J.J.M. Franse, F. Tomiyama, M. Ono, M. Date, A. Yamagishi, Physica B **177**, 223 (1992)
27. E.A. Tereshina, Y. Skourski, M. Kuzmin, M. Doerr, W. Iwasieczko, J. Wosnitza, I.S. Tereshina, J. Phys.: Condens. Matter. **29**, 24LT01-6 (2017)
28. N.H. Duc, in *Handbook on the Physics and Chemistry of Rare Earths*, vol. 24, ed. by K.A. Gschneider Jr., L. Eyring (Elsevier, Amsterdam, 1997). (Chap. 163)
29. J.J.M. France, R.J. Radwanski, in *Handbook of Magnetic Materials*, vol. 7, ed. by K.H.J. Buschow (North-Holland, Amsterdam, 1993), p. 307. (Chap. 5)
30. E.A. Tereshina, I.S. Tereshina, M.D. Kuz'min, Y. Skourski, M. Doerr, O.D. Chistyakov, I.V. Telegina, H. Drulis, J. Appl. Phys. **111**(9), 093923 (2012)
31. J.P. Liu, F.R. de Boer, P.F. de Châtel, R. Coehoorn, K.H.J. Buschow, J. Magn. Magn. Mater. **132**, 159 (1994)
32. Yu. Skourski, M.D. Kuzmin, K.P. Skokov, M. Richter, D. Eckert, I.S. Tereshina, K.-H. Müller, J. Magn. Magn. Mater. **290–291**, 435 (2005)
33. S. Sinnema, Ph.D. Thesis (University of Amsterdam, 1988)
34. K.W.H. Stevens, Proc. Phys. Soc. A **65**, 209 (1952)
35. S. Zherlitsyn, B. Wustmann, T. Herrmannsdörfer, J. Wosnitza, IEEE Trans. Appl. Supercond. **22**(3), 4300603(3) (2012)
36. E.A. Tereshina, A.V. Andreev, Intermetallics **18**, 1205 (2010)
37. E.A. Tereshina, A.V. Andreev, J. Kamarad, H. Drulis, J. Alloys Compd. **492**, 1 (2010)